Available online at www.sciencedirect.com
SCIENCE DIRECT®
Thin Solid Films 433 (2003) 50–56
thin solid films
www.elsevier.com/locate/tsf

Studies of pulsed high-current arcs used to prepare carbon films

S. Muhl[a,*], F. Maya[a], S. Rodil[a], E. Camps[b], M. Villagran[c], A. Garcia[c]

[a]*Instituto de Investigaciones en Materiales, UNAM, Mexico D.F. 04510, Mexico*
[b]*Instituto Nacional de Investigaciones Nucleares, Salazar, Mexico*
[c]*Centro de Instrumentos, UNAM, Mexico D.F. 04510, Mexico*

Abstract

Electric arcs have been widely used for the preparation of carbon films. In particular, the filtered cathode arc technique is known to be one of the best methods for the production of diamond-like carbon with high concentrations of sp^3-bonded carbon. In 1999 the possibility of producing diamond micro-crystallites [Nature 402 (1999) 162] using a high-current arc pulse, >1000 A with a 60-ms duration, between two 0.5-mm-diameter graphite rods. For such high-density plasma systems, the relative density of the deposit precursors, and their spatial variation, energy, degree of ionisation, etc. are very important, since these determine the characteristics of the deposits produced. In this paper we report optical studies involving time-resolved emission spectroscopy (identification of the emitted species at different delay times), time-resolved photography (temporal and spatial evolution of the arc) and shadowgraphy (temporal and spatial evolution of the plasma and particle formation) of a pulsed arc similar to that used in the microcrystalline diamond work. In addition, we report preliminary results of the characteristics of carbon films deposited on both a close substrate (as in the report in Nature) and on a variably biased substrate placed approximately 10 cm from the arc.

Keywords: Arc evaporation; Amorphous carbon; Raman; Shadowgraphy

1. Introduction

Carbon films can be prepared with a wide range of properties, from highly insulating to conducting, opaque to transparent, hard or soft, etc. [2,3]. The variety is possible because of the unique atomic bonding characteristics of carbon and the resultant multiplicity of morphologies that this bonding permits. If carbon deposition is carried out using hydrogen dilution and high temperatures, or using high temperatures and high pressure in the presence of a suitable catalyst, then diamond films or diamond crystals can be prepared [4,5]. Plasma decomposition of a hydrocarbon gas can be used to produce hydrogenated amorphous carbon (a-C:H) films with a range of densities and properties [2]. Sputtering of graphite with little to no ion bombardment results in amorphous sp^2-bonded carbon (a-C) coatings [3], and if adequate bombardment is used then the deposit can have up to 85% sp^3-bonded carbon and is called either diamond-like carbon (DLC) or tetrahedrally bonded carbon (ta-C) [6,7]. However, if the bombardment is excessive or the temperature is too high, then mainly sp^2 bonding and in extreme conditions micro or nanocrystalline graphite may then be obtained [8]. Thermal evaporation of graphite gives a-C, but if this is performed under moderate helium pressure then fullerenes can be obtained, and with a suitable catalyst, carbon nanotubes or nanowires [9]. Arc evaporation of graphite can result in a-C, ta-C or fullerenes, depending on the ion energy and gas pressure. Furthermore, a recent publication in *Nature* [1] indicated that high-current pulsed arc evaporation of 0.5-mm-diameter graphite rods could be used to produce microcrystalline diamonds [1]. Our work on pulsed arc evaporation has not resulted in the formation of diamond under any conditions, but it appears that both a-C and ta-C can be obtained. The present report details our characterisation of the arc used to prepare such films.

2. Experimental

Carbon deposits were prepared in a glass bell-jar vacuum system with a baffled diffusion oil pump backed

*Corresponding author. Tel.: +52-5-622-4736; fax: +52-5-616-1251.
E-mail address: muhl@servidor.unam.mx (S. Muhl).

0040-6090/03/$ - see front matter © 2003 Elsevier Science B.V. All rights reserved.
PII: S0040-6090(03)00317-1

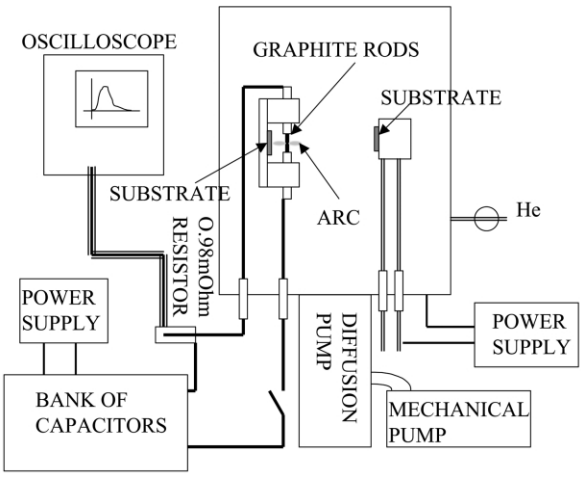

Fig. 1. Schematic representation of the experimental arrangement used.

by a single-stage mechanical primary pump. The base pressure of the system was better than 1.3×10^{-5} Pa. Graphite rods of 0.5 mm in diameter were machined from 3.12-mm-diameter high-purity AERO graphite from ESPI; the thin part of the rods was typically 5 mm long. These rods were placed in a specially designed holder such that the two opposing rods remained aligned during the arc evaporation. The copper rod holders were coupled to a bank of 15 capacitors (33 000 μF, maximum of 100 V) connected in parallel to give a total capacitance of 0.5 F. The arc was created by discharging the capacitors, which had been previously charged to the required voltage, across the graphite rods. The arc current and its temporal form were measured by detecting the voltage drop across a low-inductance 0.98-mΩ resistor in the circuit with a HP54522A digital oscilloscope. The *I*–*V* curves were analysed to determine the inductance in the circuit and the contact resistance between the carbon rods. This resistance value was then used to estimate the arc energy. A schematic drawing of the experimental arrangement is shown in Fig. 1.

Two silicon substrates were used for each experiment, one placed 8 mm from the arc and the other on a water-cooled copper block, 6 cm from the arc, which was connected to a DC power supply to bias the substrate relative to the graphite. In this way, it was possible to vary the energy of the carbon ions that were incident on the substrate during deposition.

Optical measurements of the arc consisted of rapid photography of the arc, spectrophotometry of the arc emission and shadowgraphy. A high-resolution CCD camera (Princeton Instruments, model 1024E) was used throughout, together with an Acton Research Pro-500 monochromator with a 1/8-in. quartz optical fibre bundle for spectrophotometry, and expanded red (632.8 nm) and green (543.5 nm) He–Ne lasers for shadowgraphy. To carry out the shadowgraphy, the laser light was allowed to expand to a diameter of approximately 6 cm using an optical path of ~20 m. This beam was used to illuminate the graphite rods, creating a shadow on a screen placed ~80 cm behind them. A CCD camera with a 120-mm-focal-length lens was used to record the shadows during the arc. The light for the spectral analysis was collected using a UV-Vis fibre bundle placed ~20 cm from the arc. Delay times from 10 μs to 50 ms were used to follow the temporal evolution of the emission. Different spectral windows could be observed, depending on the grating used: $\Delta\lambda = 340$ nm when a 500-g/mm grating was used, and $\Delta\lambda = 40$ nm for 1200 g/mm. The photography and spectrophotometry were performed at low pressure, $<1.3\times10^{-3}$ Pa, whereas the shadowgraphy was mainly carried out at atmospheric pressure.

Some experiments were carried out at reduced pressure in a 6-in. six-way cross-vacuum chamber with opposing glass windows to reduce the perturbation by the bell jar wall of the shadow projection. The arc radius in air was measured as a function of the pressure at a fixed arc current, and atmospheric-pressure experiments were carried out as a function of both the charging voltage and the number of capacitors.

The films produced under vacuum ($<10^{-5}$ Pa) at both substrate sites were characterised by X-ray diffraction, Raman spectroscopy and profilometry.

Preliminary measurements of the carbon ion energy and density were carried out using the temporal response of the signal of a Faraday cup-type of ion detector placed at various distances from the arc, and by normalising the temporal variation of the ion current measured to a cylindrical Langmuir probe biased to −80 V. We followed the procedure outlined elsewhere to obtain the average ion energy [10]. The electrical signal generated by the ~1200-A arc strongly interfered with these measurements and limited the use of the method.

3. Results and discussion

The experiments were of three types: (a) those carried out to duplicate, within the limits of the information provided, the conditions reported in the article in *Nature* [1] and variations of these conditions; (b) deposition of carbon, at a pressure of $<10^{-5}$ Pa, as a function of the arc and the bias applied to the substrate mounted on the copper block 6 cm from the graphite rods; and (c) optical analysis of the arc, in air, mainly at atmospheric pressure, but also as a function of the pressure.

Even though the conditions reported in *Nature* [1] were duplicated, no evidence of the formation of diamond crystals was observed. In fact, all deposits were found to be amorphous or small-grained graphite. However, the properties of the films grown on the biased holder were found to be dependent on the bias used.

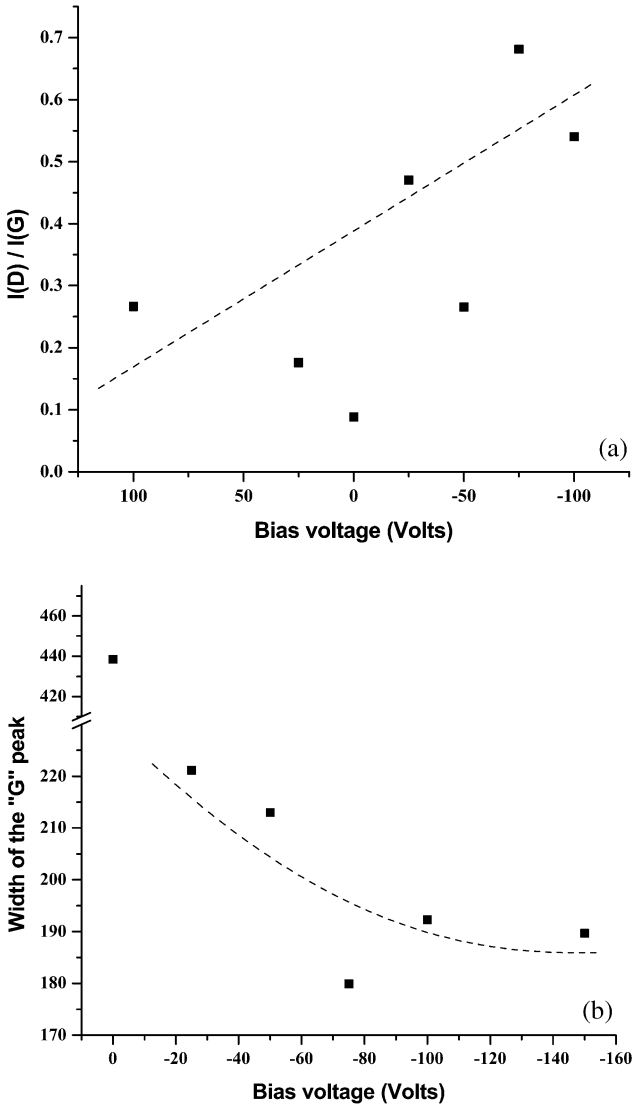

Fig. 2. Results of the Raman analysis of samples described in the text. (a) The ratio of the intensities of the D and G Raman peaks; and (b) width of the G-peak vs. the applied bias. These experiments were performed at a pressure of 10^{-5} Pa using an arc current of 1200 A.

The surface roughness decreased from 15 to 7 Å as the negative bias was increased from 0 to −80 V. Fig. 2a,b show the ratio of the intensities of the D and G Raman peaks and width of the G-peak vs. the applied bias. Based on the description of the variation of these variables provided by Ferrari and Robertson, our results are typical of carbon films with a relatively low sp^3 content; moreover, as the bias changes from negative to positive values, the amount of sp^3-bonded carbon probably increases to some extent [11]. The ion energy measurements were very difficult because of the electrical interference from the current pulse; however, the two studies indicated that the ion energy was between 250 and 280 eV. This result is in agreement with the Raman analysis, since the initial ion energy is greater than that necessary to drive sp^3 formation by subplantation, and the use of a positive bias reduces the ion energy and may be expected to increase the sp^3 fraction.

The emission of the carbon arc consists mainly of the Swan system, degraded to the violet, with band heads located at wavelengths of: 436.5 (4-2), 468.5 (6-5), 516.5 (0-0), 512.9 (1-1), 563.5 (0-1), 558.8 (1-2) and 589.9 nm (6-8) (high-pressure bands of the Swan System) (Fig. 3). The emission spectra were observed with a strong continuum background from the carbon electrodes and the hot electrons emitted. The presence of neutral carbon species could not be observed, as their emission lines coincide with those of the Swan system. No emission from C_x ($x>1$) molecular species was observed. The emission spectra were practically the same no matter what conditions were used in the experiment (i.e. the charge voltage or number of capacitors); changes in the experimental conditions affected only the intensity of the lines. Maximum emission was observed at delay times of approximately 2 ms, which is just before the maximum of the current peak of the arc, as can be observed in Fig. 5a.

Simulation of the arc I–V curves for a peak current of 1200 A indicated that the total resistance of the circuit was 0.16 Ω with inductance of 1.5×10^{-4} H. Using the resistivity measured for our graphite, 2.26×10^{-6} Ω m, we calculated a contact resistance between the graphite rods of 0.113 Ω. Therefore, the total dissipated power in the arc was approximately 163 kW.

In shadowgraphy, the scattered light intensity is proportional to the second derivative of the refractive index of the medium, and as such the method can be used to study variations in the refractive index brought about by local changes in the gas pressure, temperature or density [12]. This technique has been successfully used to study localised explosions by performing rapid photography of the expansion of the shock wave [13,14]. A typical shadow halo obtained from the arc can be observed in Fig. 4. However, as evident in Fig. 5a, the expected expansion of the halo was not observed. In fact, the radius of the halo remained almost constant for the duration of the current pulse, and the halo only expanded by a factor of two as the current decreased to zero. Therefore, we have the somewhat peculiar situation that there is an explosion that does not expand. There are two possible explications of this result. The first is that the dense arc-induced plasma allows the formation of a secondary plasma between the electrodes and it is the effective refractive index of this plasma that generates the halo. Alternatively, the carbon atoms emitted collide with the surrounding gas molecules and form clusters, which are then ejected outwards by thermal expansion of the gas. Since this process continues to occur during the lifetime of the arc, a volume of space is established around the arc site with a radially varying density of

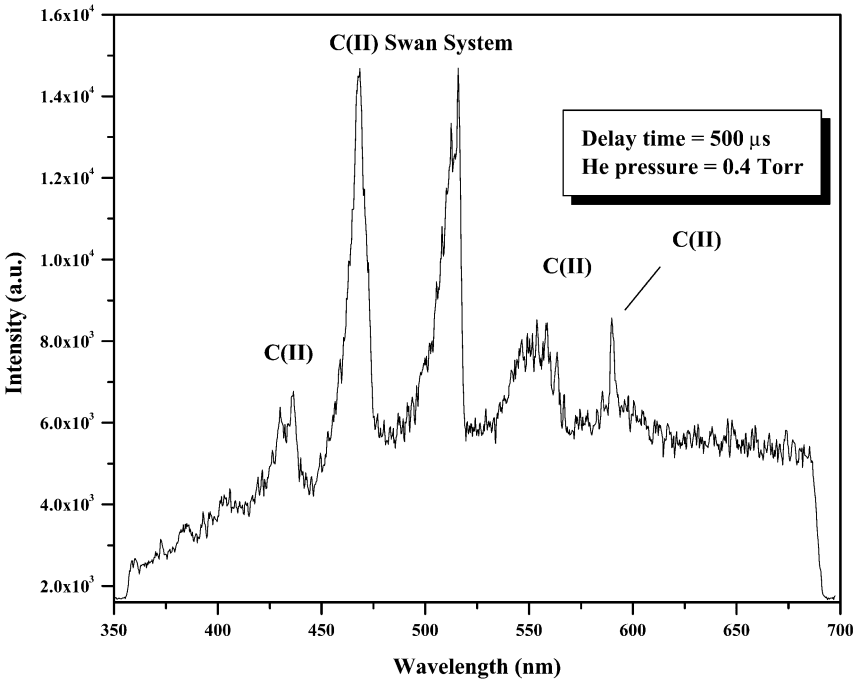

Fig. 3. Typical optical emission spectrum of the pulsed DC arc, at a pressure of 10^{-5} Pa and arc current of 1200 A.

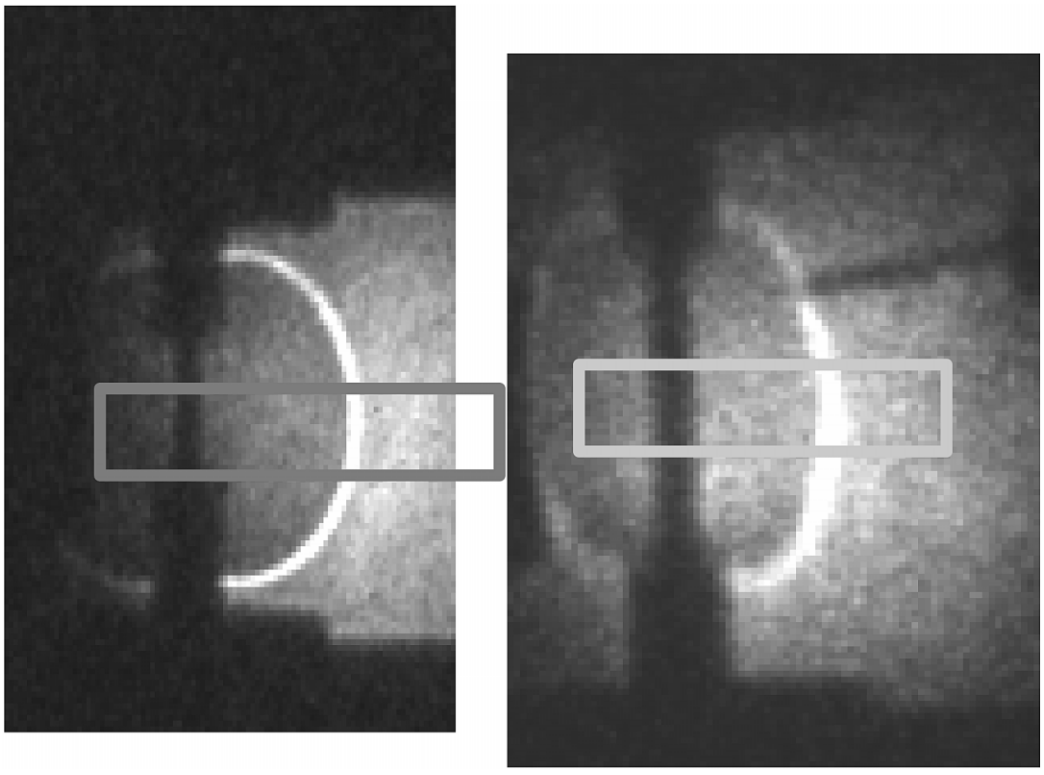

Fig. 4. Typical shadowgraphs of the arc in air at atmospheric pressure illuminated with red (623 nm) and green (543.5 nm) HeNe lasers; exposure time 10 μs and delay time 5 ms. The arc current was ~1000 A.

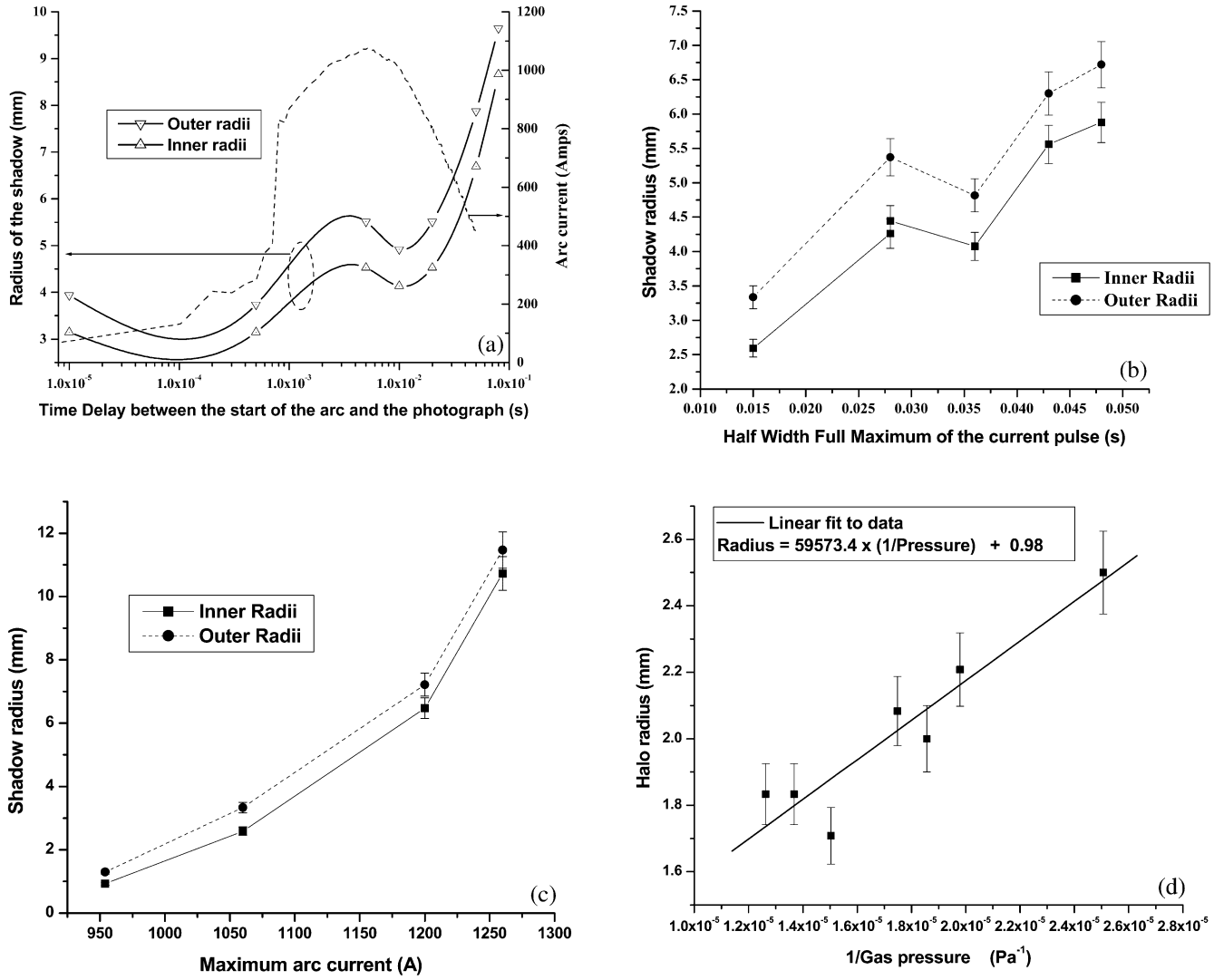

Fig. 5. Variation of the radius of the halo, obtained in air at atmospheric pressure, as a function of: (a) time; (b) full width at half-maximum of the current pulse; (c) maximum arc current; and (d) the reciprocal of the gas pressure; (a) also shows the temporal variation of the arc current. The data for (b–d) were taken at the maximum of the current pulse, i.e. at a time of 5 ms.

carbon clusters. The effective refractive index of this volume filled with gas and carbon clusters could generate the halo observed by Mie scattering of the laser light [15].

Fig. 5b,c show the variation of the radius of the shadowgraph halo as a function of the half-width at full maximum of the current pulse (the number of capacitors) and the maximum arc current (the capacitor charge voltage). The number of capacitors determines the width of the current pulse, but does not change the maximum current. The corresponding figure shows that the halo radius only changes by a factor of less than two as the pulse width increases more than four-fold. The charge voltage determines the maximum arc current, and therefore the number of carbon atoms emitted, and from the figure it can be observed that the increase in the halo radius is superlinear to this current. Fig. 5d shows that the halo radius increases almost linearly with the reciprocal of the gas pressure (or the mean free path for collisions in gases). The experiments showed that no halo was formed at pressure of $<4\times10^4$ Pa; if the plasma model were the correct explanation, then a critical pressure significantly lower than this value would be expected, since it is well known that plasma can easily be maintained at <133 Pa.

Fig. 6 shows the intensity of the shadowgraph, obtained using the red and green lasers, along the area indicated in the photographs shown in Fig. 4 of the arc using 16 capacitors and a charging voltage of 40 V. The background intensity of the laser illumination was subtracted to allow comparison of the two cases; the insert shows the temporal variation of the arc current, as well as the time at which the photograph was taken. Fig. 7 shows the second integral of the intensity of the shad-

owgraph intensity data, and is therefore the effective refractive index of the volume around the arc. The boundary conditions for these data have been taken as 2.45, the value for graphite, near the rod and 1.0, the value for air, at the greatest distance. If the scattering process were of the Raleigh type, then it would be expected that the intensity of the scattered light should be proportional to λ^{-4}. However, the ratio of the green/red intensity is 1.13 and 1.16 for the maximum and minimum, respectively. These values are close to the ratio of the inverse of the wavelengths, 1.16, and not to the fourth power of the ratio, 1.84.

The effective refractive index data were analysed using the ideas of Mie scattering of the laser light by spherical particles of graphite, and this indicated that the particle diameter was approximately 250 nm. Fig. 8 shows a micrograph of the carbon deposit produced in air using 16 capacitors and a charging voltage of 30 V. It can be observed that the deposit is in the form of carbon clusters of quite uniform size of ~100 nm. The difference in the two diameters can be accounted for by the uncertainty of the theoretical work and the small dissimilarity in the experimental conditions.

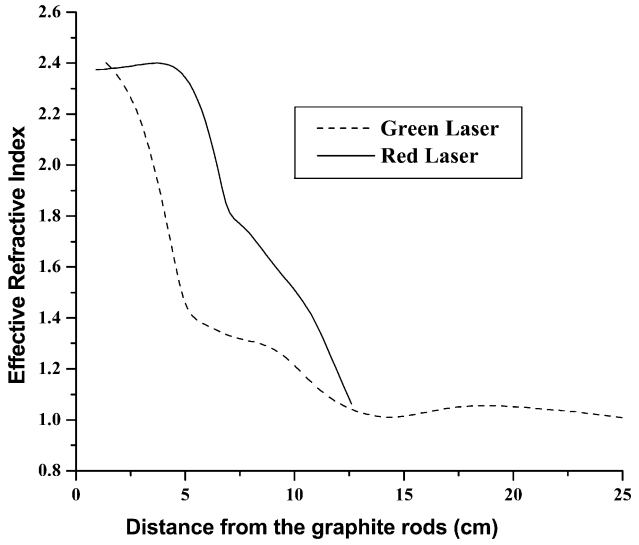

Fig. 7. Second derivative of the data shown in Fig. 6 vs. the distance from the graphite rods; thus, this is the variation of the effective refractive index of the medium around the arc.

4. Conclusion

The pulsed high-current arc evaporation of carbon resulted in amorphous deposits mainly of sp^2-bonded carbon. The as-emitted ion energy may be too large for the formation of high-quality diamond-like carbon, and further work is required using some type of ion energy filter, or biasing, to improve the quality of the films. Emission spectroscopy showed that the carbon is emitted as atoms and not as multi-atom clusters. The unexpected results from the shadowgraphy experiments in air can be explained by considering the formation of carbon clusters very close to the arc site, followed by the expansion of this cluster cloud radially from the arc. Data analysis using the ideas of Mie scattering proposed the formation of clusters of approximately 250 nm, and

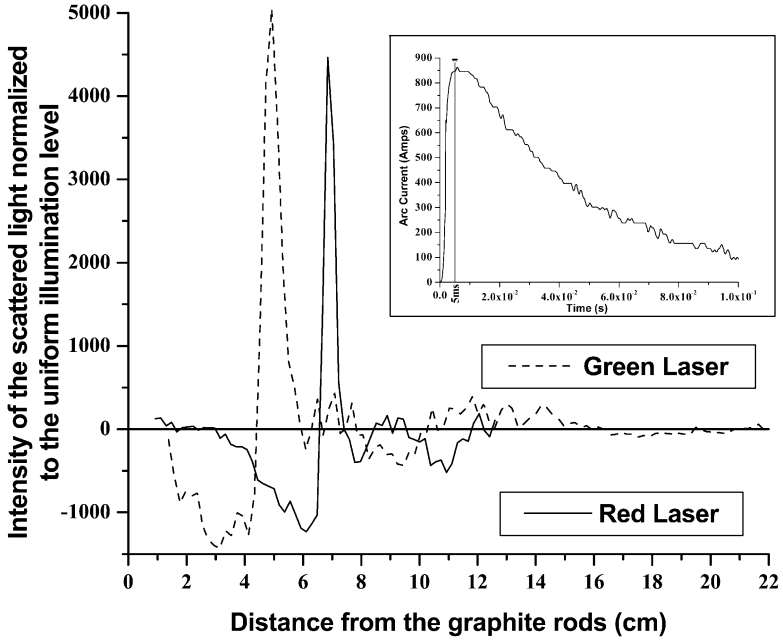

Fig. 6. The red and green light intensity, normalised to the undisturbed background level, vs. the distance from the graphite rods. The insert shows the temporal variation of the arc current.

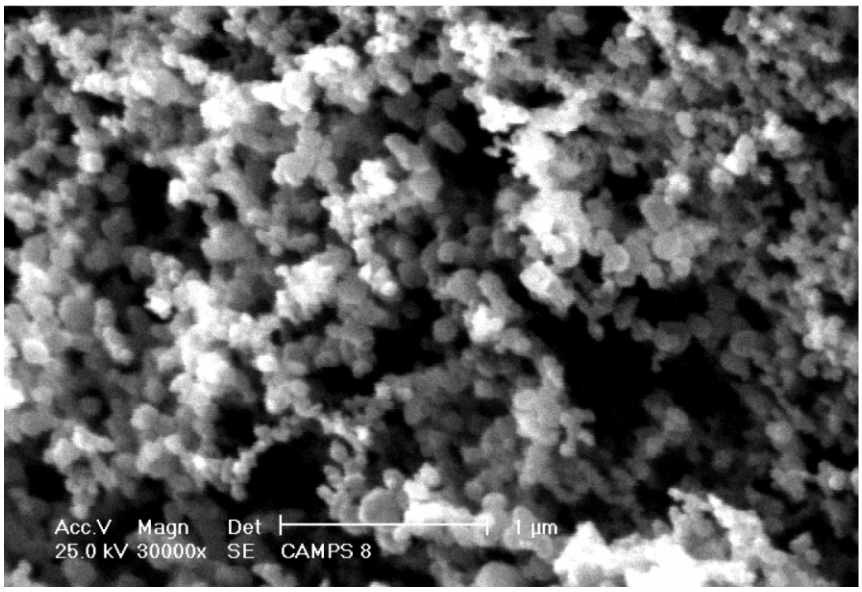

Fig. 8. Micrograph of the carbon deposit produced in air at a distance of ~0.8 cm using 16 capacitors and a charging voltage of 30 V.

observation of the deposits showed the formation of ~100-nm particles.

Acknowledgments

This work was partly supported by the projects CONACyT 27676E and DGAPA IN-103800.

References

[1] A.V. Palnichenko, A.M. Jonas, J.-C. Charlier, A.S. Aronin, J.-P. Issi, Nature 402 (1999) 162.
[2] F.G. Celi, J.E. Butler, Annu. Rev. Phys. Chem. 42 (1988) 913.
[3] J. Robertson, Mater. Sci. Eng. R 37 (2002) 129–281.
[4] J.C. Angus, H.A. Will, W.S. Stanko, J. Appl. Phys. 39 (1968) 2915.
[5] F.P. Bundy, H.T. Hall, H.M. Strong, R.H. Wentorf, Nature 176 (1955) 51.
[6] J. Schwan, S. Ulrich, H. Roth, H. Ehrhardt, S.R.P. Silva, J. Robertson, R. Samlenski, J. Appl. Phys. 70 (1996) 1416.
[7] M. Weiler, S. Sattel, K. Jung, H. Ehrhardt, V.S. Veerasamy, J. Robertson, Appl. Phys. Lett. 64 (1994) 2797.
[8] M. Chhowalla, J. Robertson, C.W. Chen, et al., J. Appl. Phys. 81 (1997) 139–145.
[9] M.S. Dresselhaus, G. Dresselhaus, P.C. Ekland, Science of Fullerenes and Carbon Nanotubes, Academic Press, London, 1996.
[10] N.M. Bulgakova, A.V. Bulgakov, O.F. Bobrenok, Phys. Rev. E 62 (2000) 5624–5635.
[11] A. Ferrari, J. Robertson, Phys. Rev. B 61 (2000) 14095–14107.
[12] R.W. Ladenburg, B. Lewis, R.N. Pease, H.S. Taylor (Eds.), Physical Measurements in Gas Dynamics and Combustion, Oxford University Press, London, 1955, p. 26.
[13] S. Siano, R. Pini, Opt. Commun. 135 (1997) 279–284.
[14] M. Villagrán Muniz, H. Sobral, E. Camps, IEEE J. Trans. Plasma Sci. 29 (4) (2001) 613–616.
[15] J. Cai, N. Lu, C.M. Sorensen, Langmuir 9 (11) (1993) 2861–2867.